

The very high-redshift Ly α forest at high resolution

George D. Becker¹†, W. L. W. Sargent¹,
and M. Rauch²

¹Palomar Observatory, California Institute of Technology, Pasadena, CA 91125, USA

²Carnegie Observatories, Pasadena, CA 91101, USA

Abstract. We present new Keck/HIRES observations of seven of the highest-redshift known quasars. These include four with $z_{\text{qso}} \geq 5.8$ and two with $z_{\text{qso}} \geq 6.3$. The data will be used to produce a complete statistical description of the Ly α forest at $z > 5$, allowing us to better assess the significance of the strong absorption seen at $z > 6.2$. We introduce the statistics of transmission gaps as a means of characterising the high-redshift evolution of the forest. In addition, we identify several clear absorption lines of low optical depth in the quasar proximity regions and briefly discuss using these to place constraints on the thermal history of the IGM at $z > 5$.

1. Introduction

The timing and mechanisms of reionisation stand among the most intriguing unknowns in the history of the early Universe. While it is certain that the bulk of the volume of the Universe must have been ionised after the epoch of recombination in order to allow transmission in the Ly α forest at $z < 6$, the nature of the reionisation process remains largely unconstrained. Polarisation measurements of the cosmic microwave background require an instantaneous reionisation event to occur after $z \sim 17$ (Kogut *et al.* 2003). However, uncertainties in reionisation models currently allow for a wide range in redshift.

Becker *et al.* (2001) and Djorgovski *et al.* (2001) first demonstrated the strong evolution of Ly α transmission towards $z > 5.7$ quasars, citing this as evidence that the tail end of reionisation may lie at $z \sim 6$. Deeper observations have confirmed that the IGM at $z > 6.2$ is highly opaque to Ly α and Ly β photons, though not all of the highest-redshift known quasars show complete Gunn-Peterson troughs (White *et al.* 2003). If some of these quasars lie in significantly neutral regions of the IGM then there must be significant variation in the ionised fraction between sight-lines.

Some alternative methods have been proposed to improve constraints on the ionisation state at $z > 6$. The luminosity function and emission line profiles of Ly α -emitting galaxies at $z \gtrsim 6.5$ suggest that the IGM may be highly ionised at those redshifts (e.g. Malhotra & Rhoads 2004; Stern *et al.* 2005). However, Ly α emission lines may be observed through a largely neutral IGM if the sources sit in sufficiently large H II regions (e.g. Santos 2004; Furlanetto *et al.* 2004). Oh & Furlanetto (2005) have extended the study of Ly α and Ly β optical depths to Ly γ , showing that the effective Ly α optical depth at $z \sim 6.2$ must be $\tau_{\text{eff}} \lesssim 15$ along at least one line of sight. Mesinger & Haiman (2004) have suggested that the greater extent of Ly β versus Ly α transmission in the region around one $z = 6.3$ quasar is due to the boundary of an H II region embedded in a largely neutral IGM. However, as Oh & Furlanetto (2005) have pointed out (and as is clear from our data), patches of Ly β transmission without corresponding Ly α are not uncommon. This effect also does not

† email: gdb@astro.caltech.edu

Table 1. $z > 5$ QSOs observed with Keck/HIRES

Name	z_{qso}	i'	z'
SDSS J1204–0021	5.09	19.3	19.0
SDSS J0915+4244	5.20	19.6	19.5
SDSS J0231–0728	5.42	19.5	19.2
SDSS J0836+0054	5.80	21.0	18.7
SDSS J0002+2550	5.82	21.5	19.0
SDSS J1030+0054	6.30	23.2	20.0
SDSS J1148+5251	6.42	23.9	20.1

appear around all $z > 6.2$ quasars, though this again may be due to patchy reionisation. Metal lines may offer a means to trace the neutral fraction over a broader dynamic range than the hydrogen Lyman series (Oh 2002), although these would simultaneously trace both the ionisation state and the amount of IGM enrichment. McQuinn *et al.* (2005) have suggested that arc-minute-scale CMB anisotropies created by H II regions via the kinetic Sunyaev-Zel'dovich effect may help to distinguish between reionisation scenarios. Finally, redshifted 21 cm emission/absorption should provide detailed information on the growth and merger of ionised regions (e.g. Tozzi *et al.* 2000; Kassim *et al.* 2004; Carilli *et al.* 2004), though these observations are still several years in the future.

Given the variety of reionisation scenarios allowed by current constraints, any new kind of observation would be highly beneficial. Since the disappearance of transmitted flux in the Ly α forest at $z > 6.2$ currently provides the strongest indication that reionisation may have lasted until $z \sim 6$, we would like to address this issue in greater detail. Songaila (2004) has looked at the evolution of transmitted flux over these redshifts and finds that it can be modelled without a sharp decrease in the ionisation rate at $z \sim 6$. However, all current work on the $z > 5$ Ly α forest has been limited to medium resolution data ($R \sim 5,000$), which is unable to capture the rich details in the narrow transmission and absorption features. Much of our understanding of the lower-redshift Ly α forest comes from high-resolution studies (e.g. Kim *et al.* 1997). A similar approach at high redshift therefore seems warranted.

2. The data

We observed seven quasars with redshifts $5.1 \leq z_{\text{qso}} \leq 6.4$ using Keck/HIRES between January and February 2005 (see Table 1). All of our objects are considerably fainter than typical sources used for high-resolution studies. The recently-upgraded detector array on HIRES was therefore essential to our programme, providing up to twice the sensitivity of the old detector in the far red. The data were reduced using the HIRES_REDUCE package written by GDB, which employs optimal sky subtraction (Kelson 2003) to remove the numerous sky emission lines. Fig. 1 compares a sample of the Ly α forest in the spectrum of SDSS J0836+0054 taken with HIRES (FWHM = 7 km s $^{-1}$) and with ESI (FWHM \approx 60 km s $^{-1}$). As expected, the higher-resolution data show numerous sharp features that have been smoothed out in the ESI spectrum.

Even at a single redshift there is significant scatter in the amount of transmitted flux and in the distribution of dark and transparent patches (see also Songaila 2004). The redshift distribution of our objects allows us to cover the Ly α forest between $z = 4.25$ and 6.20 (not including the proximity region around each quasar) with between two and five sight-lines at each redshift. The extended spectral coverage of the new detector also

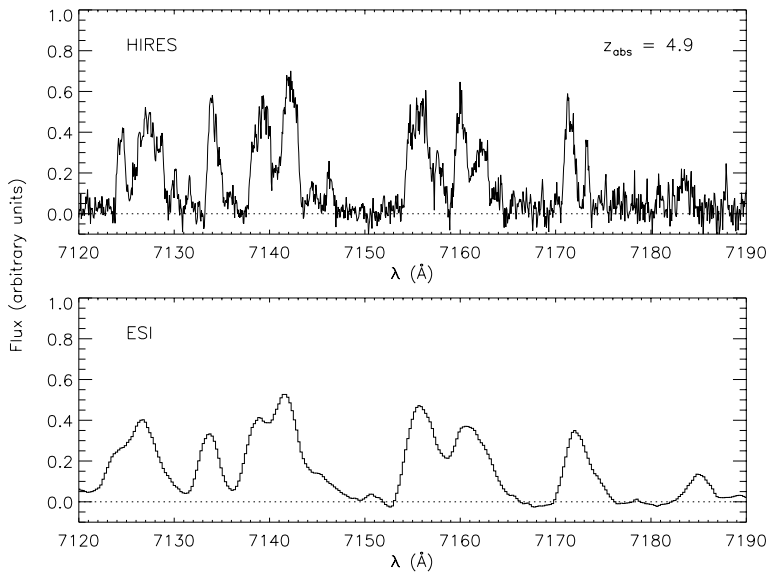


Figure 1. A sample of the Ly α forest at $z_{\text{abs}} = 4.9$ in the spectrum of SDSS J0836+0054 taken with HIRES (*top*) and with ESI (*bottom*). The ESI data were kindly provided by S. G. Djorgovski.

allows us to cover the complete Lyman series for each object down to the Lyman limit at the emission redshift.

3. Transmission gaps vs. dark gaps

At $z \gtrsim 4.5$ it becomes increasingly difficult to fit Voigt profiles to the Ly α forest without significant ambiguity. As an alternative, Songaila & Cowie (2002) measured the “dark gap” distribution function, which measures the number density of regions in the forest where the absorption is saturated. Simulations show a correlation of the length of the dark gap with the optical depth at the gap centre (Paschos & Norman 2004). However, at $z > 5$ the distribution rolls over as gaps begin to merge. At that point, a single dark gap may represent a very long section of the forest.

As a complement to dark gaps, we measured sections of the forest that show residual transmission. We have so far attempted to gain only a rough sense for the statistics of these regions. The transmission gaps were identified by eye and no attempt was made to account for incompleteness, although we used only a subset of four sight-lines with similar noise levels. Some of the properties of the transmission gaps are shown in Fig. 2. The velocity width and equivalent width of the transmission gaps show a smooth decline from $z \approx 4.1$ to 6. In contrast, the mean flux and the number of gaps per unit redshift both show a break at $z \sim 5 - 5.5$. This break can be explained by the merging of transmission gaps with decreasing redshift, similar to the merging of dark gaps towards higher redshift. However, the distribution of transmission gaps shows the clearest trend at the high-redshift limit. The decrease in the velocity width, mean flux, and number density of transmission gaps with redshift all suggest that the amount of transmitted flux in the Ly α forest should diminish smoothly from $z \sim 5$ down to zero at $z \sim 6.3$. The very strong absorption measured at $z > 6.2$ would thus be expected based on these trends.

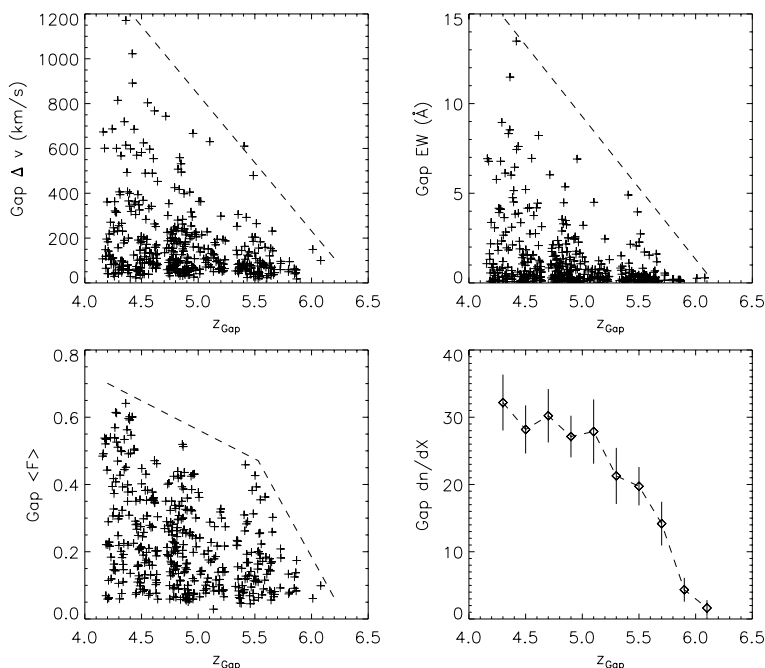


Figure 2. Ly α forest transmission gap characteristics as a function of redshift along four lines of sight. *Top left:* velocity width. *Top right:* equivalent width. *Bottom left:* mean normalised flux. *Bottom right:* number density per unit redshift path. Error bars are Poissonian. Vacant intervals in the scatter plots at $z = 4.7$ and 5.3 are due the atmospheric A and B bands. These have been taken into account to compute dn/dX . All dashed lines are drawn to guide the eye.

4. Proximity regions

Line blending makes it difficult to fit Voigt profiles to the general Ly α forest at high redshift. However, individual lines can still be seen in the proximity region immediately blue-ward of each quasar's Ly α emission line (Fig. 3). The distribution of absorption line widths has been used to demonstrate a possible thermal signature of He II reionisation at $z \sim 3$ (Schaye *et al.* 2000). Material in the proximity region will experience additional heating from the quasar. However, we can still use the available lines to set an upper bound on the temperature of the IGM under the assumption that the gas is nearly isothermal. This would be the case following a recent and abrupt reionisation event where photoionisation is the dominant heating mechanism (Hui & Haiman 2003; Theuns *et al.* 2002; but cf. Miralda-Escudé & Rees 1994).

Fig. 4 shows the distribution of b -values for lines that are well-constrained in the proximity regions of six quasars. Interloping metal lines and spurious identifications will add a small number of narrow components. The minimum b -value therefore appears to be $\sim 15 - 20 \text{ km s}^{-1}$ along each line of sight, which is similar to values found at lower redshifts. This implies that there is at least some gas at $T < 24,000 \text{ K}$ around each quasar, precluding a large temperature spike predicted in some of the most simple and extreme scenarios for reionisation at $z \sim 6.5 - 7$.

5. Conclusions

We have presented a unique data set consisting of high-resolution spectra of several of the highest-redshift known quasars. These data will be used to produce a complete

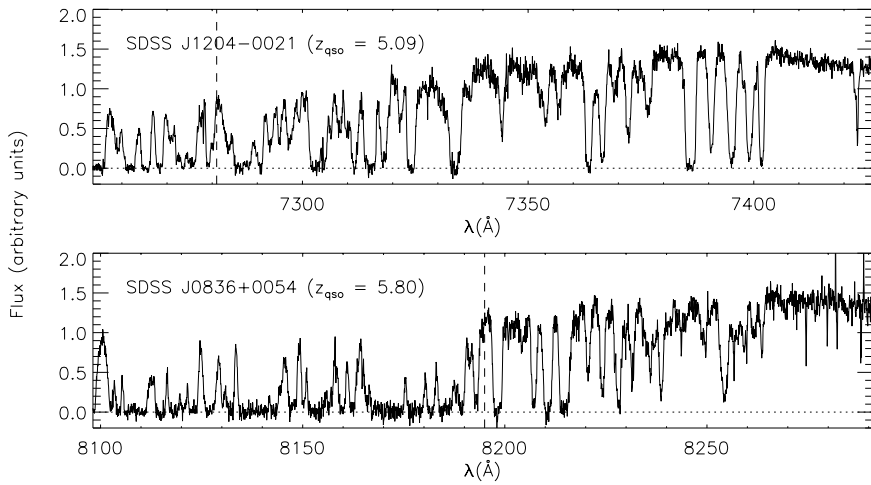


Figure 3. Quasar proximity regions along two lines of sight. Each panel spans -6000 km s^{-1} to $+1000 \text{ km s}^{-1}$ from the start of the Ly α forest. Vertical dashed lines indicate the bluest extent to which Voigt profiles have been fitted.

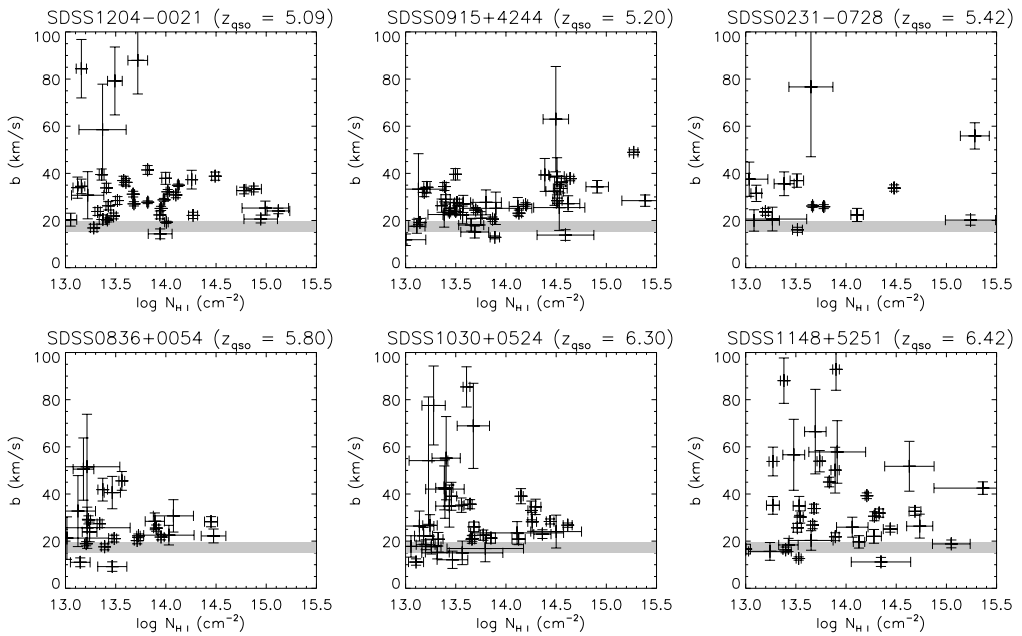


Figure 4. Voigt profile b -values versus H I column densities for well-constrained lines in the Ly α proximity regions of six quasars. The shaded areas between 15 and 20 km s^{-1} are meant to suggest a lower limit to the b -value distributions, considering the likely presence of a few lower values due to spurious fits and interloping metal lines.

statistical description of the $z > 5$ Ly α forest, enabling us to better assess the significance of the near absence of transmitted flux seen at $z > 6.2$. Statistics on the number density and characteristics of transmission gaps promise to be useful at the high-redshift end. Very preliminary work suggests that stretches of transmitted flux shrink and disappear

with redshift at a steady rate from at least $z \sim 5$ to 6.3. Finally, we have fitted Voigt profiles to lines in the quasar proximity regions in order to demonstrate the potential for placing thermal constraints on reionisation scenarios.

Acknowledgements

WLWS has been supported by the NSF through grants AST 99-00733 and AST 02-06067. MR has been supported by the NSF through grant AST 00-98492 and by NASA through grant AR-90213.01A.

References

- Becker, R. H., *et al.*, 2001, *AJ*, 122, 2850
Carilli, C. L., Gnedin, N., Furlanetto, S., Owen, F., 2004, *New Astr. Rev.*, 48, 1053
Djorgovski, S. G., Castro, S., Stern, D., Mahabal, A. A., 2001, *ApJ*, 560, L5
Furlanetto, S. R., Hernquist, L., Zaldarriaga, M., 2004, *MNRAS*, 354, 695
Hui, L., Haiman, Z., 2003, *ApJ*, 596, 9
Kassim, N. E., Lazio, T. J. W., Ray, P. S., Crane, P. C., Hicks, B. C., Stewart, K. P., Cohen, A. S., Lane, W. M., 2004, *P&SS*, 52, 1343
Kelson, D. D., 2003, *PASP*, 115, 688
Kim, T., Hu, E. M., Cowie, L. L., Songaila, A., 1997, *AJ*, 114, 1
Kogut, A., *et al.*, 2003, *ApJS*, 148, 161
Malhotra, S., Rhoads, J. E., 2004, *ApJL*, 617, L5
McQuinn, M., Furlanetto, S. R., Hernquist, L., Zahn, O., Zaldarriaga, M., 2005, *astro-ph/0504189*
Mesinger, A., Haiman, Z., 2004, *ApJ*, 611, L69
Miralda-Escudé, J., Rees, M. J., 1994, *MNRAS*, 266, 343
Oh, S. P., 2002, *MNRAS*, 336, 1021
Oh, S. P., Furlanetto, S. R., 2005, *ApJ*, 620, L9
Paschos, P., Norman, M. L., 2004, *astro-ph/0412244*
Santos, M. R., 2004, *MNRAS*, 349, 1137
Schaye, J., Theuns, T., Rauch, M., Efstathiou, G., Sargent, W. L. W., 2000, *MNRAS*, 318, 817
Songaila, A., 2004, *AJ*, 127, 2598
Songaila, A., Cowie, L. L., 2002, *AJ*, 123, 2183
Stern, D., Yost, S. A., Eckart, M. E., Harrison, F. A., Helfand, D. J., Djorgovski, S. G., Malhotra, S., Rhoads, J. E., 2005, *ApJ*, 619, 12
Theuns, T., Schaye, J., Zaroubi, S., Kim, T., Tzanavaris, P., Carswell, B., 2002, *ApJ*, 567, L103
Tozzi, P., Madau, P., Meiksin, A., Rees, M. J., 2000, *ApJ*, 528, 597
White, R. L., Becker, R. H., Fan, X., Strauss, M. A., 2003, *AJ*, 126, 1